CHAPTER II
LITERATURE REVIEWS

2.1 Artificial muscle as an actuator

Polymer artificial muscle technologies are being developed for large deformations by repetitive molecular motions that produce similar strains and higher stresses using electrostatic forces, electrostriction, ion insertion, and molecular conformational changes. There are a variety of polymers that exhibit substantial deformations in response to an applied voltage. A film fabricated from these materials reversibly contracts and expands in length and volume, and is called an actuator, behavior which is quite similar to human or animal muscles. It is interesting to compare the performance characteristics of polymer artificial muscles with natural muscles in terms of response rate, elastic modulus, strain, stress, etc. The applications of muscle-like materials are intended for medical devices, prostheses, robotics, toys, and biomimetic devices (Baughman, 1996 and Mirfakhrai *et al.*, 2007). Figure 2.1 shows three states during the electromechanical cycle of a rocking-chair-type, bimorph actuator. Electrochemical transfer of dopant (K^+) between electrodes causes bending either to the right or to the left (Baughman *et al.*, 1996).

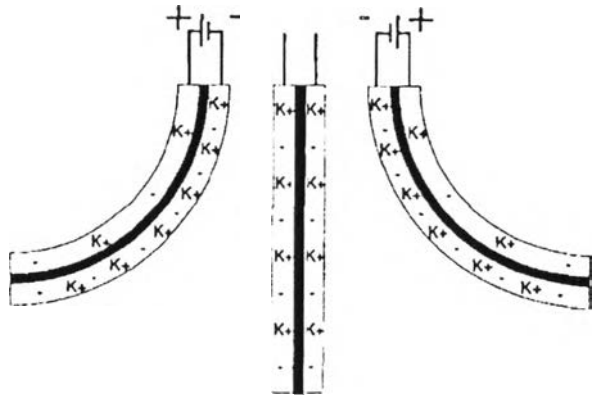

Figure 2.1 Schematic representatives of three states during the electromechanical cycle of a rocking-chair-type, bimorph actuator (Baughman *et al.*, 1996).

Moschou *et al.* (2004) prepared a novel artificial muscle based on an acrylic acid/acrylamide hydrogel blend with a polypyrrole/carbon black (Ppy/CB) composite. The material was optimized in terms of its electroactuation response by varying acrylic acid content, the blend concentration of the conductive composite, and the intensity of the electric field. The higher the acrylic acid content, the higher the bending angle of the hydrogel was obtained. They also found that the hydrogel composed of 4 %w/w carbon black alone presented a significantly lower response than its Ppy/CB counterpart. As expected, the application of higher potentials (2 and 3 V) showed improvement in the response of the material.

Moschou *et al.* (2005) also obtained improved response characteristics of the artificial muscle through optimization of the hydrogel material based on the electroactive constituents of the hydrogel precursor solution and the polymerization conditions. Hydrogels were prepared by mixing deionized water, the desired weight ratio of unsaturated aliphatic acids (acrylic acid, maleic acid, glutaconic acid, or mixtures of the above), and acrylamide, based on total monomer content and polypyrrole composite with 20 %w/w carbon black. *N,N'*-methylenebisacrylamide was used as the crosslinking agent. One way of increasing the ionic distribution in the hydrogel was to incorporate a monomer that has a higher content of charged groups per molecule. The bending angle responses increased aliphatic acid content. When the polymerization temperature of the hydrogel precursor solution was gradually increased to 45 °C and finally to 60 °C, the artificial muscle samples showed increased electroactuation responses, attributed to a decrease in the chain length of the polymer. Use of a crosslinking agent that enhanced the extent of hydrogen bonding within the hydrogel network improved mechanical stability and reproducibility of the electroactuation.

Niamlang *et al.* (2008) investigated polydimethylsiloxane (PDMS) gel as an electroactive polymer actuator. The storage modulus of PDMS gels increased linearly with crosslink density, but nonlinearly with electric field because of the increase in the number of junction points and dipole moments generating the electrostatic force within the matrices. The degree of bending and the dielectrophoretic forces of PDMS gels increased linearly with electric field strength, for a PDMS gel suspended in silicone oil between copper electrodes.

Hiamtup *et al.* (2008) studied the effects of electric field strength, particle concentration, and operating temperature on the electromechanical response of poly(dimethyl siloxane) networks containing doped polyaniline particles. The storage moduli of the composites increased when an electric field was applied because of the electrostriction effect between polarized polyaniline particles embedded in poly(dimethyl siloxane) networks. The composite film exhibited a deflection, whose magnitude increased with increasing electric field strength, but decreased slightly when the particle concentration was increased to 20 %v/v.

Thipdech *et al.* (2008) studied the electrorheological properties of acrylonitrile-butadiene rubber (NBR) and poly(3-thiopheneacetic acid)/acrylonitrile-butadiene rubber blends (P3TAA/NBR). For the pure NBR system, the storage modulus response increased with increasing electric field strength. For the P3TAA/NBR system, the storage modulus response increased with particle concentration due to particle-particle interaction under electric field. For the temporal response, both systems were irreversible because there were residual dipole moments remaining in the systems, when the electric field was off. The bending response and the dielectrophoretic force of the blend system were smaller than for the pure NBR system, because the P3TAA particles set up dipole moments in the opposite direction to those of the rubber matrix.

Thongsak *et al.* (2010) studied the electromechanical properties of styrene-isoprene-styrene (SIS) films as functions of electric field strength and temperature. The results showed the storage modulus linearly increased with temperature up to 330 K at 1 rad/s in the absence of electric field reflecting the entropic nature of the elastomeric matrices. The storage modulus response also increased with increasing of electric field up to 1 kV/mm because the applied electric field induced electrical networks within the SIS matrix.

Kunchornsup *et al.* (2012) studied physically cross-linked cellulosic gels (Phy gel), prepared by the solvent casting method using 1-butyl-3-methylimidazolium chloride (BMIMCl) ionic liquid to dissolve microcrystalline celluloses. The relative dielectric permittivity increased with increasing frequency because of the ionic polarization. The electric field induced internal dipole moments at a relatively low temperature, and the storage modulus increased. The deflection

experiment in Figure 2.2 schematically illustrates the bending of the cellulosic gel film towards the positive side under electric field strength above 100 V/mm.

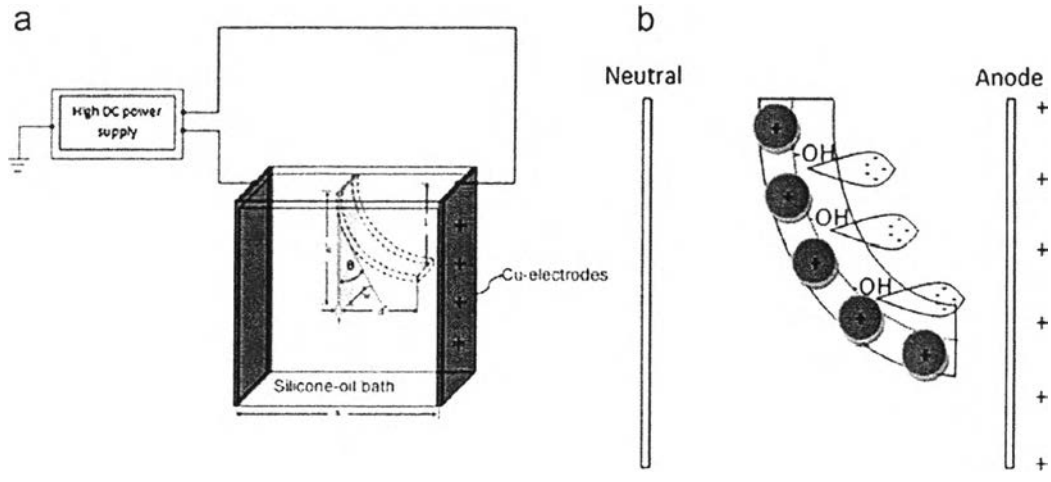

Figure 2.2 Schematic illustrations of: (a) bending response measurement of Phy gel suspended vertically in silicone-oil bath and sandwiched between copper electrodes. A DC electric field was applied horizontally at 30 ± 0.5°C causing a deflection distance, (b) actuation mechanisms were from two dominating factors; ionic polarization of $BMIM^+$ cation and electronic polarization of cellulosic hydroxyl group (Kunchornsup *et al.*, 2012).

Tungkavet *et al.* (2012) studied the electromechanical properties, thermal properties and deflection of pure gelatin hydrogels and nanowire-polypyrrole/gelatin hydrogels as functions of temperature, frequency, and electric field strength. The results showed that the storage modulus, the storage modulus response, and the storage modulus sensitivity increased with increasing electric field strength and increasing amount of nanowire-polypyrrole. It can be concluded that the interaction of electrical polarization of nanowire-polypyrrole and the effect of particles acting as fillers affected the mechanism of the storage modulus response.

2.2 Electroactive polymers (EAPs)

Electroactive polymers (EAPs) are polymers that exhibit a shape change in response to electrical stimulation and can be divided into two distinct groups: electric EAPs and ionic EAPs. Electric EAPs are very attractive in that they can perform energy conversion between the electric and mechanical forms and hence can be utilized as both solid-state electromechanical actuators and motion sensors. The electromechanical response of these polymers can be linear, as in typical piezoelectric polymers, or non-linear as in electrostrictive polymers which exhibit the Maxwell stress effect induced response. In contrast, ionic EAPs are driven by diffusion of ions and require an electrolyte for the actuation mechanism. Examples of ionic EAPs are gels, polymer-metal composites, conductive polymers, and carbon nanotubes (Bar-Cohen, 2004; Shahinpoor *et al.*, 2007).

The following literature review describes examples of electroactive polymers and their applications;

Prissanaroon *et al.* (2000) studied the effects of dodecylbenzene sulfonic acid (DBSA) as a dopant on electrical conductivity of polypyrrole films in N_2 and SO_2 atmosphere. The polypyrrole films doped with DBSA can be used to detect small low levels of SO_2. The short-time conductivity response of the conductive films can be improved by higher doping levels or by exposure to higher SO_2 concentrations. However, below a critical doping level, the gas sensitivity was independent of the doping level. Above the critical doping level, the gas sensitivity increased to a maximum and then slightly decreased while the dopant concentration was increased.

Wichiansee *et al.* (2009) synthesized poly(3,4-ethylenedioxy thiophene)/poly(styrene sulfonic acid) (PEDOT/PSS) via the chemical oxidative polymerization and mixed with ethylene glycol (EG) to improve the electrical conductivity. Furthermore, the PEDOT/PSS/EG particles were used for studying the electrorheological properties by blending with poly(dimethyl siloxane) (PDMS) as potential actuator materials. The results showed that EG particles became polarized and induced dipole moments were generated, leading to intermolecular interactions along the direction of electric field. Moreover, adding EG increased the particle

electrical conductivity through the conformational change of the PEDOT chains and affected the electrorheological properties of PEDOT/PSS blends.

Chansai *et al.* (2009) prepared a conductive polymer-hydrogel blend between sulfosalicylic acid-doped polypyrrole (Ppy) and poly(acrylic acid) (PAA) and used as a carrier/matrix for the transdermal drug delivery under applied electric field. The effect of cross-linking ratio and electric field strength on the diffusion of the drug from PAA and Ppy/PAA hydrogels were studied. It can be concluded that, by varying the cross-linking density, the electric field strength, the drug size, the hydrogel matrix mesh size, the drug-matrix interaction, and the presence of a conductive polymer, the drug release can be controlled towards a desired level.

2.3 Conductive polymers

In 1976, Heeger *et al.* synthesized conjugated conducting polyacetylene when acetylene monomer was doped with iodine and bromine vapour. The result was that electrical conductivity became higher 10 times than the polymer prepared from undoped monomers. Due to the alternating single and double bonds in the polymer chain, the π-electrons delocalize through the whole system and become charge carriers making the polymer conductive (Harun, 2007).

Because of the large energy separation (more than 3 eV) between the valence band and the conduction band, it is necessary to subject the polymers to a transformation process called "doping" to get them to their conductive state. The doping process in conductive polymers can be carried out either chemically (through the employment oxidizing or reducing agents) or electrochemically. Thus, the unique feature of conducting polymers is that they combine the properties of two classes of materials: plastics and metals. The potential result is a material with the chemical and mechanical attributes of polymers and the electronic properties of metals or semiconductors (Formmer, 1986; Bar-Cohen, 2004).

- N-doping: partial reduction of the neutral polymer chains to generate polyanions and simultaneous insertion of compensating cations to neutralize the negative charges created in the polymers.

- P-doping: partial oxidation of the neutral polymer chains to generate polycations and simultaneous insertion of compensating anions to neutralize the positive charges created in the polymers.

In the case of polyacetylene, shown in Figure 2.3, when polarons and bipolarons are produced along the doping process, the cations are not bound to each other and can freely separate along the polymer chain causing solitons. Soliton formation results in the creation of new localized electronic states that appear in the middle of the energy gap. At high dopant levels, the charged solitons interact with other to form a soliton band which can be eventually merged with the conduction band to create true metallic conductivity (Pratt, 1996).

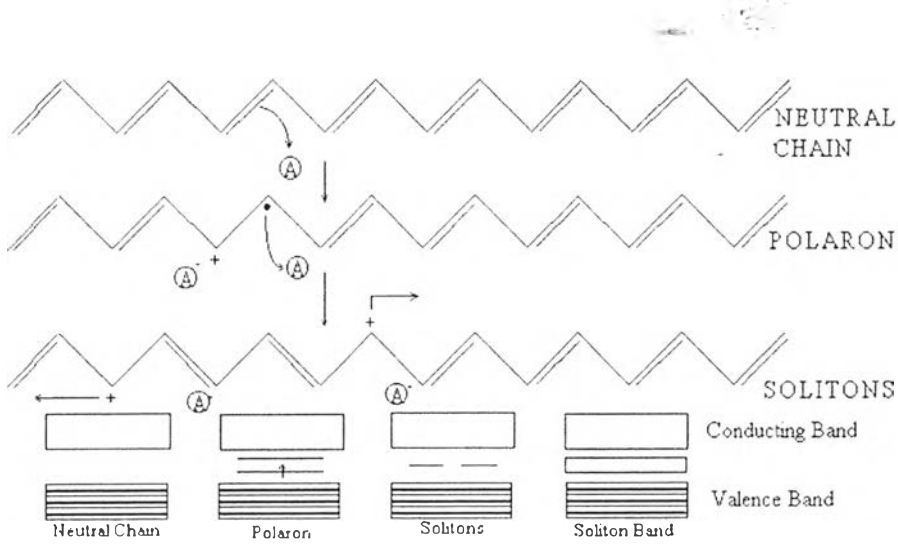

Figure 2.3 Mechanism of polyacetylene when becomes doped (Pratt, 1996).

There are other classes of conductive polymers based on different aromatic monomers such as pyrrole, thiophene, aniline, azulene, carbazole, etc. and their derivatives which have been studied with a view to improvements in both properties and applications (Bar-Cohen, 2004).

2.4 Polycarbazole

Polycarbazole is polymerized from carbazole monomers, which are aromatic heterocyclic organic compound. Carbazole itself has a tricyclic structure consisting

of two six-membered benzene ring fused on either side of a five-membered nitrogen containing ring. Polycarbazole has been employed in several applications, such as light-emitting diodes, electrochromic displays, organic transistors, and rechargeable batteries. The carbazole unit is very interesting for the following reasons:

1. 9H-carbazole is a very inexpensive starting material.
2. It is a fully aromatic unit providing a better chemical and environmental stability.
3. The nitrogen atom can be easily substituted with many functional groups helping polymer solubility, optical, and electrical properties.
4. It processes a bridged biphenyl unit resulting in a material with a lower band gap than poly(p-phenylene).

Since the carbazole unit can be polymerized at the 3- and 6- positions to yield poly(3,6-carbazole) derivatives, as shown in Figure 2.4, due to the extreme reactivity of these positions, as well as at the 2- and 7- positions to provide poly(2,7-carbazole) derivatives, as shown in Figure 2.5, with different properties and wide range of the applications (Morin *et al.*, 2007).

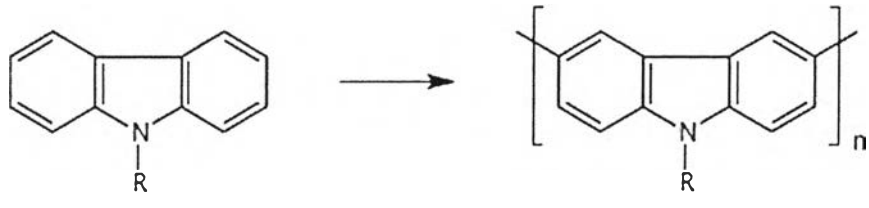

Poly(3,6-carbazole)

Figure 2.4 Chemical structure of Poly(3,6-carbazole) and its starting materials.

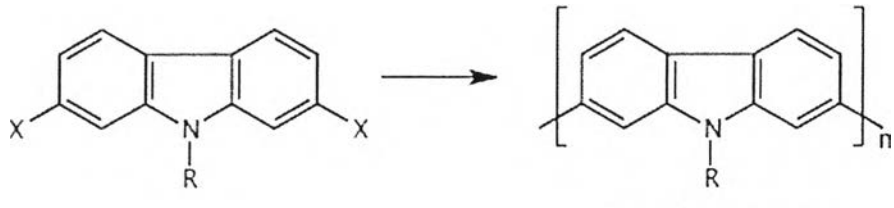

Poly(2,7-carbazole)

Figure 2.5 Chemical structure of poly(2,7-carbazole) and its starting materials.

There are two major methods to polymerize polycarbazole: chemical polymerization and electrochemical polymerization. Through chemical polymerization, monomers react with an excess amount of oxidant in a suitable

solvent. The polymerization takes place spontaneously. Electrochemical polymerization involves use of working and reference electrodes, immersed into a solution containing diluted monomer and electrolyte (dopant) in the solvent. After applying the voltage, a polymer film immediately forms on the electrode surface in one step. The chemical route is the most suitable route for large scale production, yielding polymer having a higher molecular weight with the possibility to control morphology, and there is no need to get rid of impurities that arises in the electrochemical polymerization (Harun *et al.*, 2007, Raj *et al.*, 2010, and Gupta *et al.*, 2010).

The following literature survey reviews work on the polymerization of poly(3,6-carbazole) and the mechanism of doping process;

Verghese *et al.* (1995) studied the preparation, the electroactivity, the doping/undoping reactions of polycarbazole, and the effect of pH of the medium on the properties of polycarbazole, while emphasizing the similarity of polycarbazole to polyaniline. Polycarbazole film was electrochemically prepared by the potentiostatic oxidation in a CH_3OH-$HClO_4$ mixture. The electrochemical oxidation of carbazole, shown in Figure 2.6, produced initially the 3,3'-dicarbazyl radical cation that underwent further oxidation at the same potential and couples to give polymeric products with the elimination of protons. Electrical conductivity of the synthesized polycarbazole yielded values around 10^{-4} S/cm.

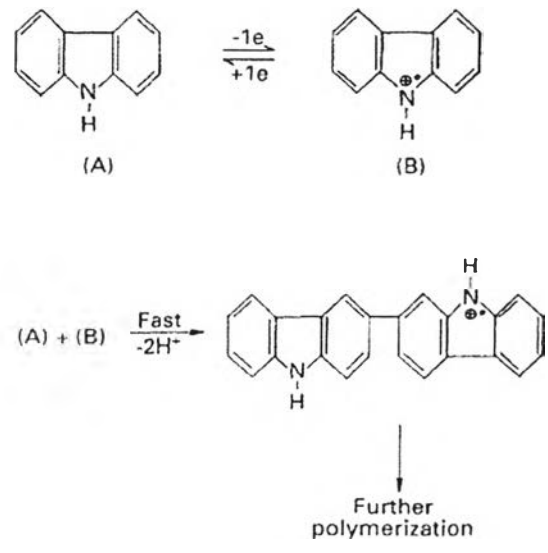

Figure 2.6 The mechanism of formation of polycarbazole (Verghese *et al.*, 1995).

Abthagir *et al.* (1998) studied the time and temperature dependences of conductivity to understand the aging process and the mechanism of conduction. The conductivity of polycarbazole perchlorate was found to be 5×10^{-4} S/cm at the temperature range of 308-450 K. The results showed that the thermal reaction involved with the elimination of dopant, followed by the degradation of the polymer backbone.

Taoudi *et al.* (2000) compared the properties and the morphology of polycarbazole obtained by the electrochemical polymerization of monomers in solution and in thin film form by the thermal evaporation on the electrode. The solution used was acetonitrile and water containing tetraethylammonium perchlorate as the electrolyte. The room temperature electrical conductivity obtained from thin film sample was 1.5×10^{-5} S/cm and 5×10^{-7} S/cm in the case of solution sample. The results showed not only polycarbazole thin films obtained by the electrochemical oxidation of vacuum predeposited carbazole monomers films, but also the polymerization efficiency was better than that obtained by the polymerization of carbazole monomers in solution in the electrolyte.

Inzelt (2003) studied the formation and the redox behavior of polycarbazole prepared by electropolymerization of solid carbazole crystals. The results showed

that, during the polymerization, anions and water molecules entered into the surface layer. However, these species left the film after the reduction of the polymer formed. The redox processes in Figures 2.7 and 2.8 were accompanied by a color change from a pale yellow/colorless (reduced) to a dark green (oxidized) form. The comparison of the mass change and the amount of charge consumed during the reversible redox transformations of the polymer suggested that the oxidation of the polymer involved a mixed cationic and anionic charge transport, i.e. the desorption of H^+ ions and the sorption of ClO_4^- ions.

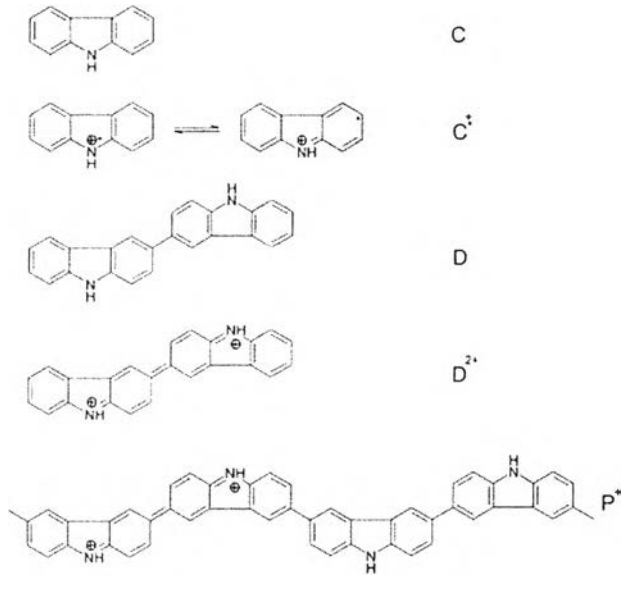

Figure 2.7 The structure of carbazole (C) and its oxidation products: C^+ is cation radical, D and D^{2+} are dimer and dimer dication, respectively, and P^+ is the half-oxidized polymer (Inzelt, 2003).

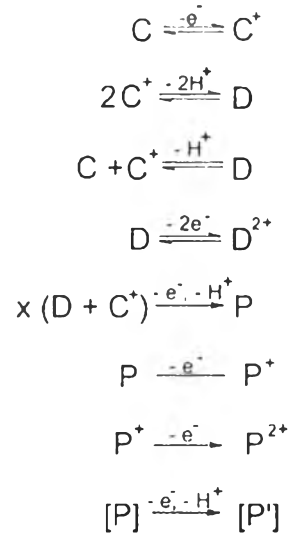

Figure 2.8 Scheme of the oxidation, and demerization of carbazole as well as the redox transformations of the dimer/polymer (Inzelt, 2003).

Siove *et al.* (2004) synthesized poly(3,6-carbazole), as illustrated in Figure 2.9, from 1,4,5,8,9 pentamethylcarbazole with $FeCl_3$ as the oxidizing agent in chloroform solution via the traditional chemical route. They also studied the effect of the amount of $FeCl_3$ on both the polymerization yield and the molecular weight of the soluble polymer fractions. Upon addition of larger excess of $FeCl_3$ proportion, polymer gel increased possibly because of the extra oxidation involving intra-chain coupling via the 2,7 tertiary carbons. Furthermore, the polymerization required theoretically at least two $FeCl_3$ equivalents with respect to monomers.

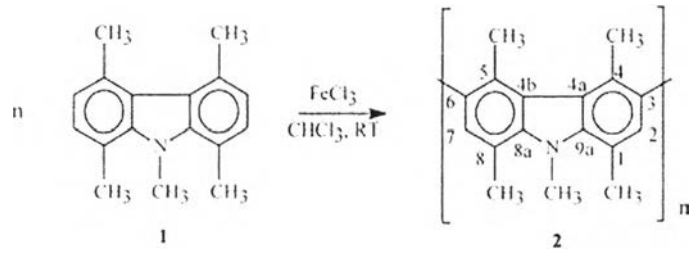

Figure 2.9 Synthesis of poly(1,4,5,8,9-pentamethyl-3,6-carbazolylene **2** by oxidative polymerization with $FeCl_3$ of pentamethylcarbazole **1** (Siove *et al.*, 2004).

Abthagir *et al.* (2004) prepared polycarbazole electrochemically in CH_3OH-$HClO_4$ mixture and studied the charge transport and their thermal properties. The result showed that the conductivity gradually increased with increase temperature up to 413 K, where a maximum value of 1.27×10^{-3} S/cm was observed. The nature and the chemical reactivity of the dopant, the process of doping, the doping level, and the polymer crystallinity were found to play a vital role in controlling the conductivity. Thus, the conduction process in polymers was a complex phenomenon.

Macit *et al.* (2004) studied electroinitiated and polymerized polycarbazole in acetonitrile using tetrabutylammonium tetrafluoroborate (TBAFB) by the direct electron transfer via the constant potential electrolysis based on an anodic peak potential. It had been observed that polymer yield increased with time, monomer concentration, and polymerization potential. According to the electrochemical polymerization mechanism as shown in Figure 2.10, carbazole was first oxidized at the anode, giving 3,3'-dicarbazyl cation, and the polymerization proceeded in successive steps. Also, the electrical conductivities were measured to be about 10^{-3}-10^{-4} S/cm and increased with decreasing temperature.

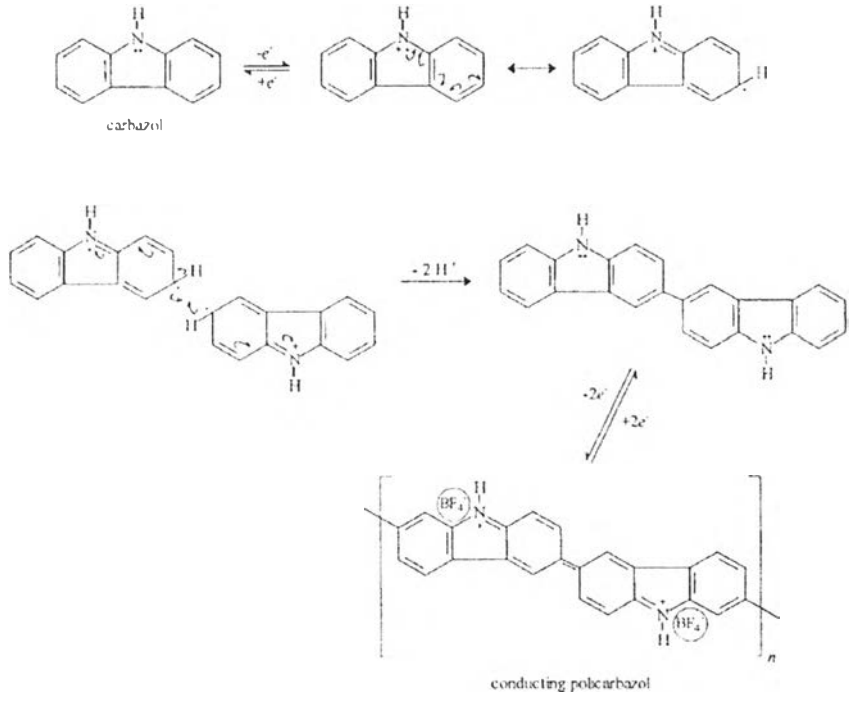

Figure 2.10 Proposed mechanistic scheme for the electropolymerization of carbazole (Macit *et al.*, 2004).

Zhuang *et al.* (2009) investigated electropolymerized polycarbazole on indium tin oxide electrodes in two air- and water-stable room temperature ionic liquids, 1-butyl-3-methylimidazolium hexafluorophosphate (BMI-PF_6) and N-butyl-N-methylpyrrolidinium bis((trifluoromethyl)sulfonyl)imide (BMP-TFSI) using cyclic votammetry, potentiostatic electrolysis, and potentiostatic pulse electrolysis. The polymer films showed electrochromic behavior. The electrical conductivity of the polycarbazole films obtained from BMP-TFSI was 4.52 ± 0.45 mS/cm, whereas the electrical conductivity of films obtained from BMI-PF_6 was 11.5 ± 1.48 mS/cm.

Gupta *et al.* (2010) studied the effect of supporting electrolytes on electropolymerization, redox property, impedance, and crystallinity of polycarbazole. Two different supporting electrolytes tetrabutylammonium perchlorate ($TBAClO_4$) and tetrabutylammonium tetrafluoroborate ($TBABF_4$) dissolved in acetonitrile were used for the synthesis of polycarbazole. The results showed that $TBAClO_4$ was a better supporting electrolyte than $TBABF_4$. The conductivity of polycarbazole-$TBAClO_4$ and polycarbazole-$TBABF_4$ were 9.54×10^{-2} and 20.44×10^{-3} S/cm, respectively.

Raj *et al.* (2010) synthesized polycarbazole by the chemical polymerization in acetonitrile using ammonium persulfate as an oxidant. The selection of solvents, concentration of the monomer, composition of the solvent, polymerization time, temperature, and pH were optimized to obtain better quality and yield of the polycarbazole. The FT-IR spectra showed that polycarbazole seems to be essentially composed of the recurring carbazole 2,5-diyl unit. The electrical conductivity was maximum at 8.2×10^{-5} S/cm at 65 °C.

Gupta *et al.* (2010) polymerized polycarbazole with controlled morphology using the interfacial polymerization. The interfacial polymerization was performed at room temperature using ammonium peroxodisulfate as the oxidant dissolving in HCl. A solution of carbazole monomer in dichloromethane was added in the aqueous solution. Thin films were observed at the interface which later diffused into the non-aqueous phase. Radical cations were formed by the oxidation of the monomers at the micelles near the interface and grown inside the micelles. It had been proposed that the spherical micelles formed in the reaction might be regarded as a soft template in forming hollow spheres.

2.5 Purification of silk fibroin and formation of silk hydrogel

Silk fibers from silkworm (Bombyx mori) are about 10-25 μm in diameter and consist of two protein components: fibroins consist of light (~25 kDa) and heavy (~350 kDa) polypeptide chains, which are present in a 1:1 ratio and linked by a single disulfide bond. The amino acid composition of silk fibroin consists primarily of glycine (Gly) (43 %), alanine (Ala) (30 %), and serine (Ser) (12 %), which are composed of a primary structure illustrated in Figure 2.11. The other component is sericin, which is a hydrophilic protein coated on the fibroin chains (Kaplan *et al.*, 1998; Zhou *et al.*, 2000).

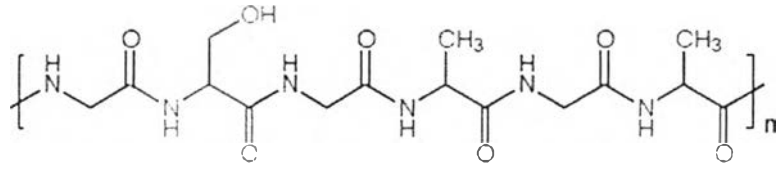

Figure 2.11 Primary structure of silk fibroin, $(Gly\text{-}Ser\text{-}Gly\text{-}Ala\text{-}Gly\text{-}Ala)_n$.

Generally, silks are composed of β-sheet structures due to the dominance of hydrophobic domains consisting of short side-chain amino acid in the primary sequence. These structures permit tight packing of stacked sheets of anti-parallel chains of the protein. Large hydrophobic domains interspaced with smaller hydrophilic domains foster the assembly of silk and the strength and resiliency of silk fibers (Bini *et al.*, 2004). Silks represent a unique family of structural proteins that are biocompatible, degradable, and mechanically superior, offer a wide range of properties, are amenable to aqueous or organic solvent processing and can be chemically modified to suit a wide range of applications (Vepari *et al.*, 2007).

Three silk fibroin morphologies have been reported: silk I, silk II, and silk III. The silk I structure is the water-soluble natural from of fibroin, and via exposure to heat or physical spinning, easily converted to the silk II structure. The fibroin protein consists of layers β-sheet structures which are asymmetrical with one side occupied by hydrogen side chains from glycine and the other occupied by the methyl side chains from alanine that produce hydrophobic domains. The β-sheet structure is

arranged so that the methyl groups and the hydrogen groups of opposing sheets interact to form the intersheet stacking in the crystals. Strong hydrogen bonds and Van der Waals forces generate the structure which is thermodynamically stable. The silk II structure excludes water and is insoluble in several solvents including mild acid and alkaline condition, and several chaotropes. The silk III structure is considered as an air/water assembled interfacial silk with helical structure (Kaplan *et al.*, 1998).

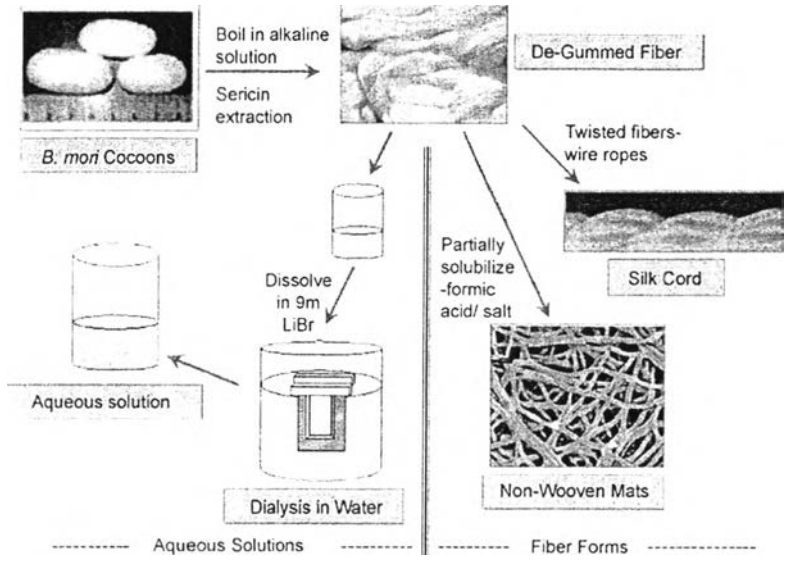

Figure 2.12 Silk fibroin is purified from sericins by boiling in alkaline solution. The de-gummed or purified silk fibers can be processed into silk cords and non-woven silk mat (Vepari *et al.*, 2007).

Hydrogels are three-dimensional polymer networks, which are formed by physical or chemical crosslinks of homopolymers or copolymers, which can be swollous media (Deligkaris *et al.*, 2010). Silk fibroin hydrogels have been prepared from an aqueous silk fibroin solution forming a β-sheet structure. Hence, there are many parameters that can affect the gelation, such as pH, temperature, concentration of fibroin solution, etc.

Kim *et al.* (2004) studied the environmental factors that influenced silk fibroin sol-gel transitions and used the osmotic stress to generate highly concentrated

fibroin aqueous solutions. The results showed that gelation of silk fibroin aqueous solution was affected by temperature, Ca^{2+}, pH, and poly(ethylene oxide) (PEO). Gelation time decreased with increase in silk fibroin concentration, decrease in pH, increase in temperature, addition of Ca^{2+}, and addition of PEO.

Matsumoto *et al.* (2006) studied silk fibroin sol-gel transitions by monitoring the process under various physicochemical conditions. The overall independencies of processing parameters including silk fibroin concentration, temperature, and pH on gel formation and protein structure can be related to primary sequence-specific features in the molecular organization of the fibroin protein. It is possible that some hydrogen bonding and electrostatic interactions were also responsible for the gelation process at the early states, but they were likely less contributory to the transition than the dominating hydrophobic interaction. The localized dehydration process resulted in the irreversible β-sheet formation due to the thermodynamic stability of the secondary structure.

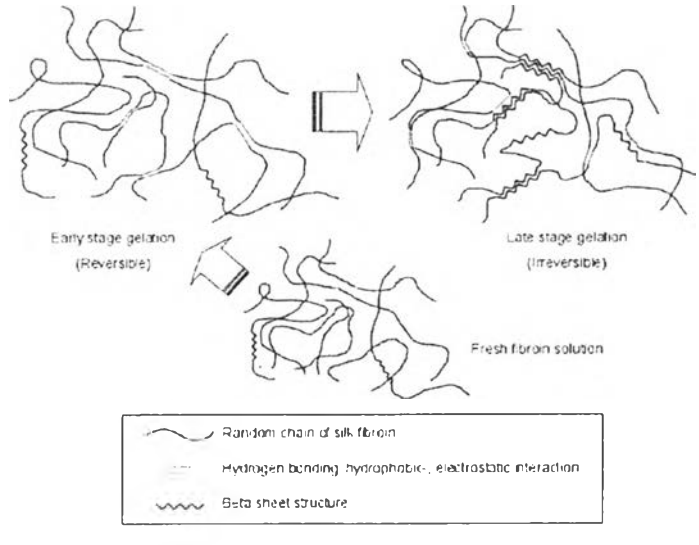

Figure 2.13 Schematic illustrations of pregelation and early and late stages of fibroin gelation, a three-stage model. A fresh solution (pregelation) has about 20 % content of β-sheet structures with negligible intermolecular bindings. Gelation is initially induced by weaker interchain interactions such as hydrogen bonding, hydrophobic interactions, and electrostatic interactions. The β-sheet structures occur

in the phase transition resulting in stable and essentially irreversible intermolecular structures (Matsumoto *et al.*, 2006).

Wang *et al.* (2008) reported a novel method to accelerate the process and control silk fibroin gelation through ultrasonication, as illustrated in Figure 2.14 Depending on the sonication parameters, including power output and time, along with silk fibroin concentration, the gelation could be controlled from minutes to hours. Mechanistically, the ultrasonication initiated the formation of the β-sheet by the alteration in hydrophobic hydration, thus accelerating the formation of physical cross-links responsible for gel stabilization. During the sonication process, the solution temperature increased from room temperature to 40-70 °C for a short period of time, which reflected a transient spike in local temperature.

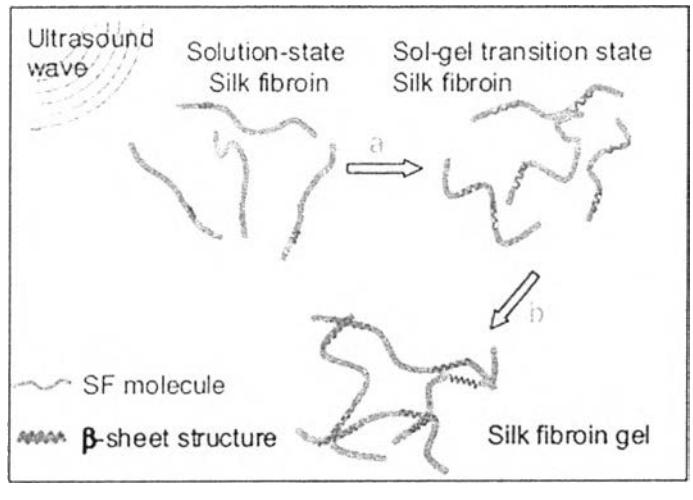

Figure 2.14 Schematic illustration of mechanism of silk gelation. The gelation process contains two kinetic steps: (a) structural change from random coil to β-sheet with some interchain physical crosslinks occurring in a short timeframe; (b) β-sheet structure extended, large quantity of interchain β-sheet crosslinks formed, and molecules organized to gel network over a relative long timeframe (Wang *et al.*, 2008).

Lu *et al.* (2011) studied the mechanism of silk electrogelation (e-gel) process as shown in figure 2.15. The gel formed at the positive electrode within the seconds of the application of the voltage. The formation almost stopped after 3 min following the decrease in current. e-Gel formation resulted in a decrease in random coil content and a significant increase in γ-helix. These results suggested intermediate conformations rather than β-sheet formation in the silk e-gel. Importantly, these results also indicated that the transformation from random coil to intermediate structures might be critical for electrogelation.

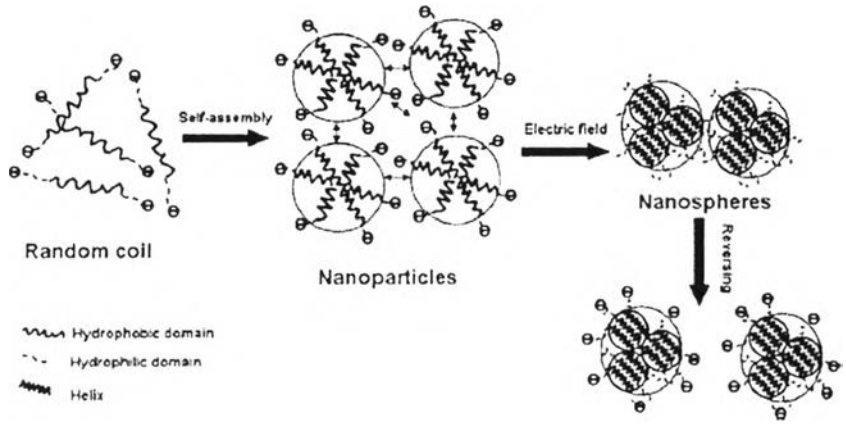

Figure 2.15 Electrogelation mechanisms. Silk fibroin firstly assembled into nanoparticles with a size of tens of nanometers and then further aggregated into microspheres with a size up to macrometers. In reversing the process the microspheres dispersed into solution rather than separated into nanoparticles (Lu *et al.*, 2011).

Nogueira *et al.* (2011) prepared silk fibroin hydrogel from the dialysis of a silk fibroin metastable solution. The hydrogels produced during the dialysis process had a cylindrical form, molded by the dialysis membrane shape. Hydrogels formed at 20 °C were physically and chemically characterized because hydrogels formed at lower temperature required long dialysis time and others formed at temperature higher than 20 °C were fragile and did not withstand handling. The β-sheet conformation was formed during silk fibroin solution gelation, as a result of silk

fibroin molecular chain dehydration and their intra and intermolecular hydrogen bond formations.

Numata *et al.* (2011) developed a facile and quick method to regulate the bulk water content of silk hydrogels by adjusting the concentrations of silk proteins, which was useful to investigate the effects of the state of water in polymeric hydrogel on its biological function. Gelation of silk fibroin was induced with ethanol and its gelation behavior was analyzed by rheometry. The results showed that melting temperature and enthalpy of fusion of the bulk water in the silk hydrogel significantly decreased with an increase in the concentration of silk proteins. While bound water were almost invariable throughout the range of concentrations, indicating that the concentration of silk protein in the hydrogel was capable of controlling the contents of water molecules in the silk hydrogel.